Journal of Power Sources 234 (2013) 201–207

Contents lists available at SciVerse ScienceDirect

Journal of Power Sources

journal homepage: www.elsevier.com/locate/jpowsour

Short communication

Improvement of long-term cycling performance of $Li[Ni_{0.8}Co_{0.15}Al_{0.05}]O_2$ by AlF_3 coating

Sang-Hyuk Lee [a], Chong Seung Yoon [b], Khalil Amine [c,*], Yang-Kook Sun [a,*]

[a] Department of Energy Engineering, Hanyang University, Seoul 133-791, South Korea
[b] Department of Materials Science and Engineering, Hanyang University Seoul, 133-791, South Korea
[c] Chemical Sciences and Engineering Division, Argonne National Laboratory, 9700 South Cass Avenue, Lemont, IL 60439, USA

HIGHLIGHTS

- The surface of NCA ($Li[Ni_{0.8}Co_{0.15}Al_{0.05}]O_2$) was coated by AlF_3 through dry process.
- The AlF_3-coated NCA full cell showed excellent electrochemical performance.
- The AlF_3-coated NCA had better thermal stability than the pristine electrode.
- AlF_3 coating suppressed the increase in resistance and particle pulverization.

ARTICLE INFO

Article history:
Received 15 December 2012
Accepted 10 January 2013
Available online 1 February 2013

Keywords:
Layered materials
Cathode materials
Dry coating
Lithium-ion batteries

ABSTRACT

The surface of a $Li[Ni_{0.8}Co_{0.15}Al_{0.05}]O_2$ cathode material was coated by a 50-nm thick AlF_3 layer using a simple dry coating process. Although the initial discharge capacity of pristine and AlF_3-coated $Li[Ni_{0.8}Co_{0.15}Al_{0.05}]O_2$ was nearly same, the AlF_3-coating significantly improved the electrochemical performances of $Li[Ni_{0.8}Co_{0.15}Al_{0.05}]O_2$ in a full cell configuration (graphite anode), especially at an elevated temperature (55 °C). Furthermore, the AlF_3-coated $Li[Ni_{0.8}Co_{0.15}Al_{0.05}]O_2$ had better thermal stability than the pristine electrode. The improved electrochemical performance likely arose from the AlF_3 coating layer which may have retarded the transition metal dissolution from HF attack. Electrochemical impedance spectroscopy and transmission electron microscopy provided direct evidence that the AlF_3 coating layer suppressed the increase in charge transfer resistance and cathode material pulverization during cycling.

Published by Elsevier B.V.

1. Introduction

The demand for power sources in portable devices, hybrid electric vehicles (HEVs) and electric vehicles (EVs) increases every year. To become viable sources of electrical power, batteries need to possess a large capacity, an excellent rate capability, be safe, and must be inexpensive [1–3]. To date, the lithium-ion battery satisfies most of these requirements, but an improvement in the components of the cathode material is still needed. Nickel-rich $Li[Ni_{1-x}M_x]O_2$ (M = Co, Mn, Al, etc.) materials are considered to be the most promising cathode materials owing to their high specific capacity which is greater than 200 mA h g^{-1} [4,5]. Among these promising materials, the $Li[Ni_{0.8}Co_{0.15}Al_{0.05}]O_2$ cathode material shows improved electrochemical performance and thermal safety with cation substitution of Co and Al by increasing the structure stability [6,7]. However, the $Li[Ni_{0.8}Co_{0.15}Al_{0.05}]O_2$ material shows poor cycle durability especially at an elevated temperature (e.g., 55 °C) because the highly delithiated $Li_{1-\delta}[Ni_{0.8}Co_{0.15}Al_{0.05}]O_2$ contains a high concentration of unstable Ni^{4+} ions and will easily transform to a more stable NiO on the cathode surface, which results in high interfacial resistance and eventual capacity fading [8]. In addition, the accompanying oxygen evolution from the delithiated $Li_{1-\delta}[Ni_{0.8}Co_{0.15}Al_{0.05}]O_2$ causes poor safety of cathode.

One effective approach to solve these aforementioned problems is coating the $Li[Ni_{0.8}Co_{0.15}Al_{0.05}]O_2$ cathode material with a uniform layer of nanoscale metal oxides [9–11], metal hydroxide [12], metal fluoride [13,14], and metal phosphates [15,16]. The coated cathode material showed a much improved capacity retention, rate capability, and even thermal stability. These coating layers may serve as i) a HF scavenger that reduces the acidity of non-aqueous electrolyte and suppresses metal dissolution from the cathode materials; and

* Corresponding authors.
E-mail addresses: amine@anl.gov (K. Amine), yksun@hanyang.ac.kr (Y.-K. Sun).

0378-7753/$ – see front matter Published by Elsevier B.V.
http://dx.doi.org/10.1016/j.jpowsour.2013.01.045

ii) as a physical protection layer of the cathode surface from HF attack and electrolyte decomposition that impedes a side reaction [17]. To date most of the coated cathode materials are based on the wet process that uses aqueous or nonaqueous solvents (mostly alcohol) which are both costly and flammable. Moreover, these wet-coating techniques require additional and complicated coating processes of mixing, drying, and heating as well as a special facility which translate into a higher production cost for the cathode material. The high production cost in this process is not widely acceptable in practical applications. Hence, a simple dry-coating process has been recently reported and is garnering attention [18,19].

Herein, a simple dry-process was developed to coat an ultrathin AlF_3 layer on a $Li[Ni_{0.8}Co_{0.15}Al_{0.05}]O_2$ cathode material based on high-speed mechanofusion without any solvent. The electrochemical performance of an AlF_3-coated $Li[Ni_{0.8}Co_{0.15}Al_{0.05}]O_2$ cell was characterized and compared with a pristine $Li[Ni_{0.8}Co_{0.15}Al_{0.05}]O_2$ cell in a full cell configuration using MCMB as an anode to accurately evaluate the coating effect. To elucidate the improved electrochemical performance of the C/AlF_3-coated $Li[Ni_{0.8}Co_{0.15}Al_{0.05}]O_2$ cell, X-ray diffraction (XRD), electrochemical impedance spectroscopy (EIS) and transmission electron microscopy (TEM) were used to characterize the electrode in detail.

2. Experimental

Nano-sized AlF_3 powder was synthesized using $Al(NO_3)_3\cdot 9H_2O$ and NH_4F with a molar ratio of 1:7. An aqueous NH_4F solution was added drop by drop into an aqueous $Al(NO_3)_3\cdot 9H_2O$ solution in which the pH was adjusted to 10. The mixed solution was aged for 5 min at 25 °C and the solvent was evaporated. The obtained $(NH_4)_3AlF_6$ powders were heated at 400 °C for 5 h in continuously flowing nitrogen and AlF_3 powders were obtained.

The $[Ni_{0.8}Co_{0.15}Al_{0.05}](OH)_2$ precursor was prepared by a co-precipitation method [20]. An aqueous solution of $NiSO_4\cdot 6H_2O$, $CoSO_4\cdot 7H_2O$ and $Al_2(SO_4)_3\cdot 16H_2O$ was pumped into a continuously stirred tank reactor (CSTR, capacity of 4 L) with a N_2 atmosphere. At the same time, a NaOH solution and a desired amount of NH_4OH solution were fed separately into the reactor. To synthesize the $Li[Ni_{0.8}Co_{0.15}Al_{0.05}]O_2$, a mixture of $[Ni_{0.8}Co_{0.15}Al_{0.05}](OH)_2$ with $LiOH\cdot H_2O$ was calcined at 780 °C for 15 h under a steady flow of oxygen. To coat the surface of the $Li[Ni_{0.8}Co_{0.15}Al_{0.05}]O_2$, 5 g of AlF_3 (1 wt%) was mixed thoroughly with 500 g of $Li[Ni_{0.8}Co_{0.15}Al_{0.05}]O_2$ powder *via* a Nobilta (NOB-130, Hosokawa Micron Co., Japan) for 5 min at a speed of 3400 rpm.

Powder X-ray diffraction (XRD, Rigaku, Rint-2000) employing Cu-Kα radiation was used to identify the crystalline phase of the prepared powder at each stage. The XRD data were obtained at $2\theta = 10°–80°$, with a step size of 0.03° and a count time of 5 s. From XRD data, the lattice parameters were calculated by a least-squares method. The morphology of the powders was determined with scanning electron microscopy (SEM, S-4800, Hitachi). The surface of the AlF_3-coated powder was also observed using transmission electron microscopy (TEM, JEOL 2010).

The electrochemical performance of the synthesized cathodes was assessed in a 2032 coin-type cell. The cell consisted of a cathode and a lithium metal anode separated by a porous polypropylene film. The cathode was fabricated with a mixture of prepared powder, carbon black, polyvinylidene fluoride in *N*-methyl-2-pyrrolidone. The slurry was spread onto aluminum foil and dried in a vacuum oven at 110 °C. The electrolyte used was 1 M $LiPF_6$ in a 1:1 volume mixture of ethylene carbonate and diethyl carbonate (PANAX ETEC Co., Ltd, Korea). The cells were charged and discharged by applying a constant current density of 100 mA g^{-1} (0.5 C rate) at 55 °C in the 2.7–4.3 V range.

Cells were charged to 4.3 V and opened in an Ar-filled dry box for differential scanning calorimetry (DSC) experiments. Samples of 3–5 mg were collected in a stainless steel sealed pan with a capacity of 30 μL and a gold-plated copper seal capable of withstanding a pressure of 150 atm. Thermal stability was determined in a differential scanning calorimeter (DSC, 200PC, Netzsch, Germany) using a temperature scan of 1 °C min^{-1}. The weight was constant in all cases, indicating that no leaks occurred during the experiments.

Long cycle-life tests were performed in a laminated-type full cell wrapped with an Al pouch. Mesocarbon microbeads (MCMB) were used as the anode electrode material. Cell fabrication was completed in a dry room. The cells were charged and discharged between 3.0 and 4.2 V by applying a constant 1 °C rate (200 mA g^{-1}) at 25 °C and 55 °C. AC-impedance measurements were performed using an impedance analyzer (IM6, Zahner Elektrik) over a frequency range from 1 MHz to 1 mHz with an amplitude of 10 mV_{rms}. Transmission electron microscopy (TEM) was used to observe the morphology of cycled electrodes.

To measure the extent of dissolution of elemental Ni, Co, and Al, a full cell was charged to 4.2 V and then carefully disassembled to obtain the active materials, which were subsequently stored in the electrolyte at 55 °C for four weeks. The amount of dissolved Ni, Co, and Al was measured by inductively coupled plasma (ICP-AES, PerkinElmer, Optima-4300 DV).

3. Results and discussion

Scanning electron microscopy (SEM) images of the $Li[Ni_{0.8}Co_{0.15}Al_{0.05}]O_2$ powders are shown in Fig. 1. The pristine $Li[Ni_{0.8}Co_{0.15}Al_{0.05}]O_2$ had a clean and rough spherical surface consisting of nanoparticles, whereas the AlF_3-coated sample was completely covered by an AlF_3 layer with a thickness of 50 nm, as shown in Fig. 1f. This confirmed the competency of the simple dry-coating process using the Nobilta in fully coating the surface of the $Li[Ni_{0.8}Co_{0.15}Al_{0.05}]O_2$ with an AlF_3 layer. As anticipated, this coating layer should improve electrochemical performances of $Li[Ni_{0.8}Co_{0.15}Al_{0.05}]O_2$ by protecting its surface from HF attack.

Fig. 2 illustrates the initial charge/discharge curves of Li/pristine and AlF_3-coated $Li[Ni_{0.8}Co_{0.15}Al_{0.05}]O_2$ cells at a current density of 20 mA g^{-1} (0.1 C-rate) between 2.7 V and 4.3 V at 55 °C. Both cells demonstrate almost a similar discharge capacity of 200 mA h g^{-1}. The cycling performance of Li/pristine and AlF_3-coated $Li[Ni_{0.8}Co_{0.15}Al_{0.05}]O_2$ cells over 100 aggressive cycles (voltage between 2.7 and 4.3 V, current density of 100 mA g^{-1} (0.5 C-rate) and temperature of 55 °C) are shown in Fig. 3. As expected, the AlF_3-coated $Li[Ni_{0.8}Co_{0.15}Al_{0.05}]O_2$ showed improved cycling performance exhibiting capacity retention of 84.7% compared to that of pristine $Li[Ni_{0.8}Co_{0.15}Al_{0.05}]O_2$ (79.1%). The capacity retention was similar to the that of a previous AlF_3-coated Li $[Ni_{0.8}Co_{0.15}Al_{0.05}]O_2$ material prepared by a wet-coating process [13,14].

The long-term cycling performance was evaluated using a laminated-type full cell (25 mA h capacity) with mesocarbon microbeads (MCMB, graphite) as an anode. The full cells were charged and discharged for 1000 cycles at current density of 190 mA g^{-1} (1 C-rate) and 25 °C between 3.0 and 4.2 V as shown in Fig. 4. The cycling performance of the AlF_3-coated Li $[Ni_{0.8}Co_{0.15}Al_{0.05}]O_2$ significantly improved, showing a capacity retention of 86.2% after 1000 cycles, while the pristine electrode illustrated a slow decrease in capacity, leading to a capacity retention of only 66.5% during the same cycling period.

To investigate the AlF_3 coating effect further, the cells of C/pristine and AlF_3-coated $Li[Ni_{0.8}Co_{0.15}Al_{0.05}]O_2$ were cycled over 500 cycles at 55 °C and the results are shown in Fig. 5. The C/pristine Li

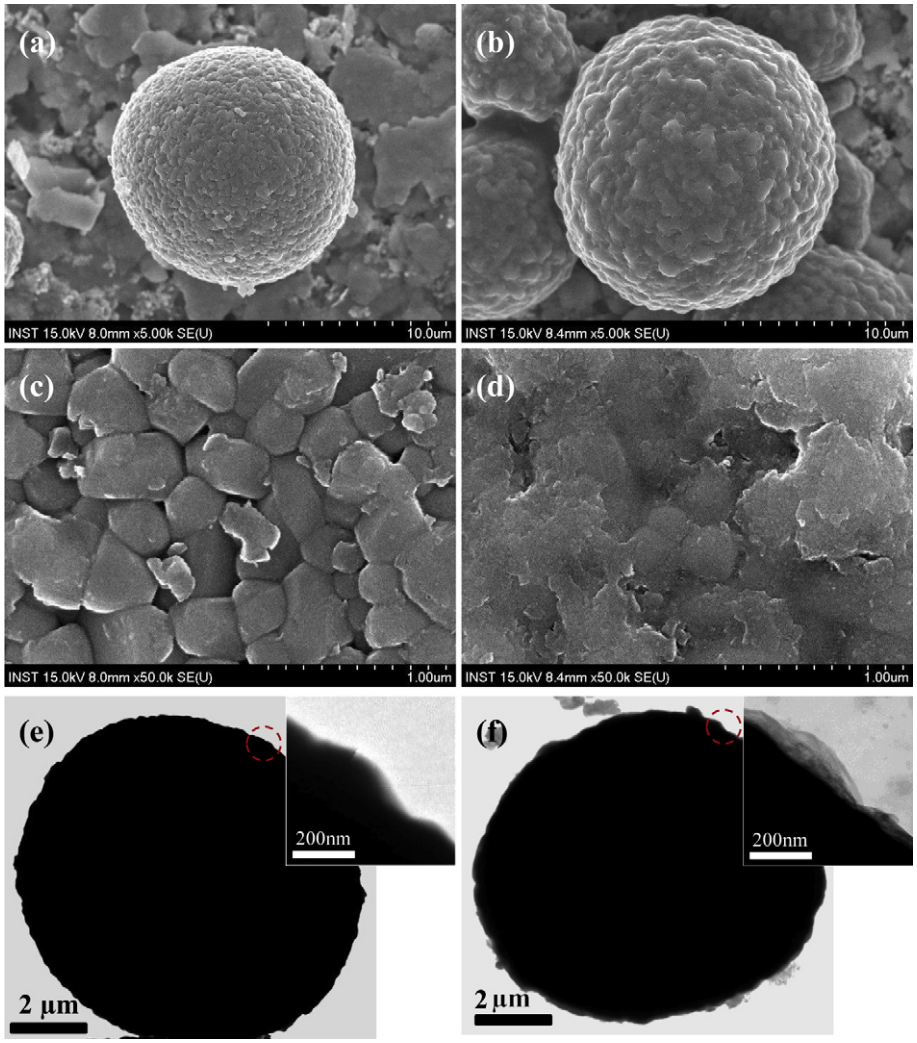

Fig. 1. SEM images of (a) the pristine $Li[Ni_{0.8}Co_{0.15}Al_{0.05}]O_2$, (c) magnified images of (a), (b) the AlF_3-coated $Li[Ni_{0.8}Co_{0.15}Al_{0.05}]O_2$, and (d) magnified images of (b). TEM images of (e) the pristine $Li[Ni_{0.8}Co_{0.15}Al_{0.05}]O_2$ and (f) the AlF_3-coated $Li[Ni_{0.8}Co_{0.15}Al_{0.05}]O_2$. TEM image in inset confirms existence of the AlF_3 coating layer (50 nm) on the surface of $Li[Ni_{0.8}Co_{0.15}Al_{0.05}]O_2$ particle.

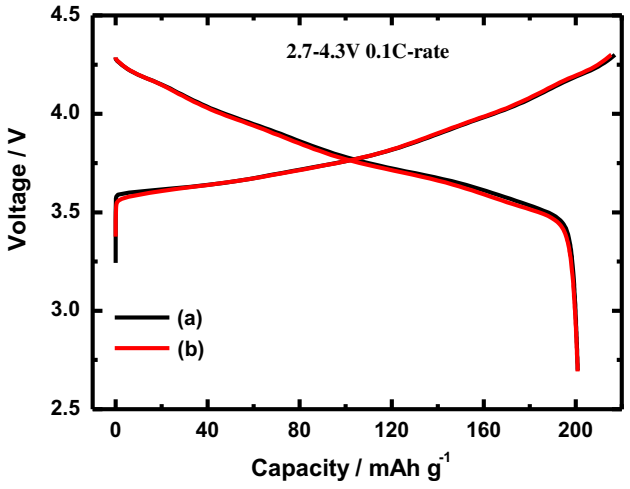

Fig. 2. Comparison of the first charge and discharge curves of (a) Li/pristine $Li[Ni_{0.8}Co_{0.15}Al_{0.05}]O_2$ and (b) Li/AlF_3-coated $Li[Ni_{0.8}Co_{0.15}Al_{0.05}]O_2$ cells at 55 °C.

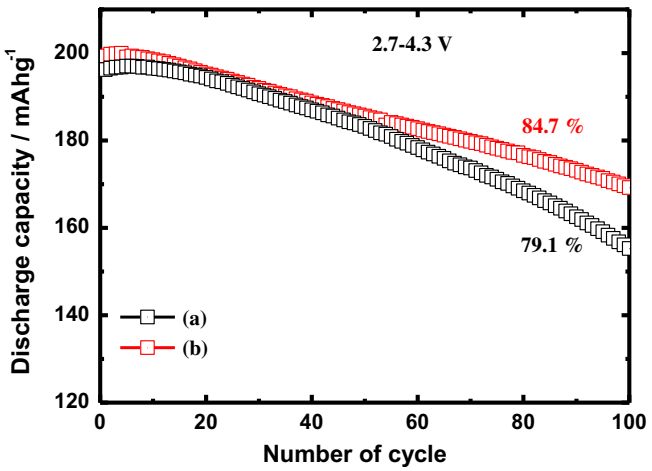

Fig. 3. Cycling performance of (a) Li/pristine $Li[Ni_{0.8}Co_{0.15}Al_{0.05}]O_2$ and (b) Li/AlF_3-coated $Li[Ni_{0.8}Co_{0.15}Al_{0.05}]O_2$ cells during 100 cycles at a current density of 100 mA g^{-1} (0.5 C) at 55 °C.

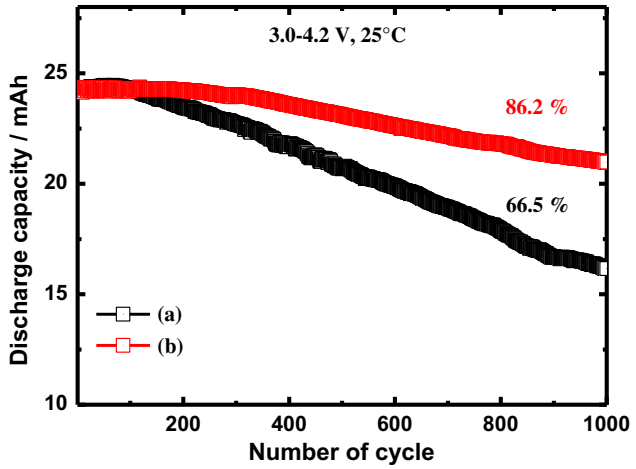

Fig. 4. Cycling performance of (a) C/pristine $Li[Ni_{0.8}Co_{0.15}Al_{0.05}]O_2$ and (b) C/AlF_3-coated $Li[Ni_{0.8}Co_{0.15}Al_{0.05}]O_2$ cells during 1000 cycles at a current density of 190 mA g^{-1} (1.0 C) at 25 °C.

$[Ni_{0.8}Co_{0.15}Al_{0.05}]O_2$ exhibited a rapid capacity loss, leading to a capacity retention of only 11.7%. This poor performance was ascribed to the instability of the Ni-rich layered host structure caused by multiple phase transitions [21,22] and transition metal dissolution of cathode surface resulting from HF attack which causes severe serrations of the cathode particle surface [23]. However, C/AlF_3-coated $Li[Ni_{0.8}Co_{0.15}Al_{0.05}]O_2$ demonstrates a greatly improved cycling performance, exhibiting a capacity retention of 55.9% due to complete encapsulation of the particle surface with an AlF_3 layer.

To further evaluate the AlF_3 coating effect, the rate capability property was investigated for the C/pristine and AlF_3-coated $Li[Ni_{0.8}Co_{0.15}Al_{0.05}]O_2$ cells shown in Fig. 6. Each cell was charged at a current density of 100 mA g^{-1} (1 C-rate) before the discharge test and then discharged at a current density from 200 mA g^{-1} (1 C-rate) to 1400 mA g^{-1} (7 C-rate). As observed, at a low C-rate, both cells showed similar Li^+ intercalation stability. However, the C/AlF_3-coated $Li[Ni_{0.8}Co_{0.15}Al_{0.05}]O_2$ cell exhibits a higher discharge capacity than the pristine cell at a higher current rate of 5 C and 7 C, indicating that the AlF_3 layer does not hinder the diffusion of the Li^+ ion. Another interesting feature is the C/pristine $Li[Ni_{0.8}Co_{0.15}Al_{0.05}]O_2$ which shows capacity decline at higher current rate, especially

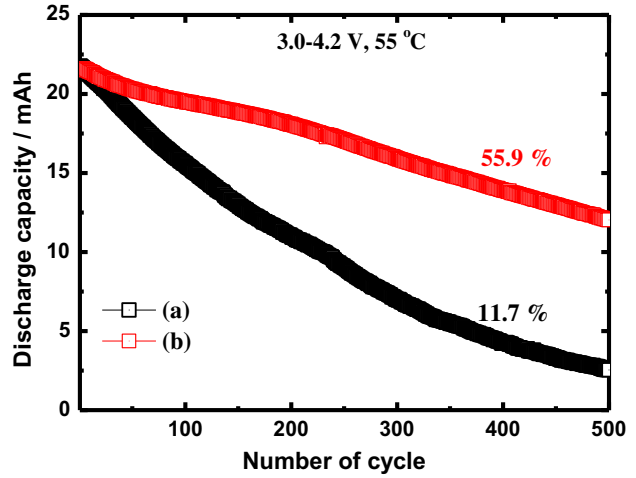

Fig. 5. Cycling performance of (a) C/pristine $Li[Ni_{0.8}Co_{0.15}Al_{0.05}]O_2$ and (b) C/AlF_3-coated $Li[Ni_{0.8}Co_{0.15}Al_{0.05}]O_2$ cells during 500 cycles at a current density of 200 mA g^{-1} (1.0 C) at 55 °C.

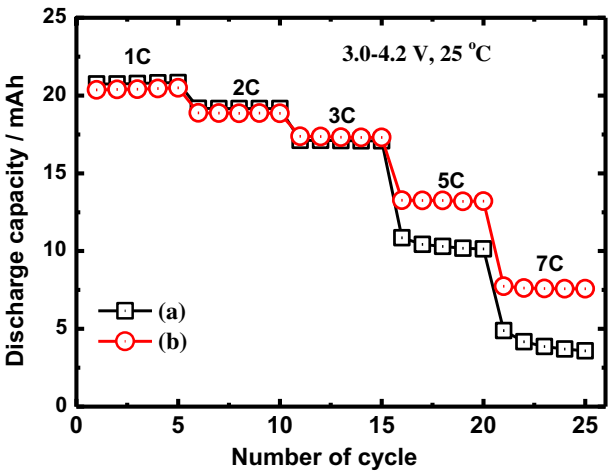

Fig. 6. Rate capability of (a) C/pristine $Li[Ni_{0.8}Co_{0.15}Al_{0.05}]O_2$ and (b) C/AlF_3-coated Li $[Ni_{0.8}Co_{0.15}Al_{0.05}]O_2$ at 25 °C.

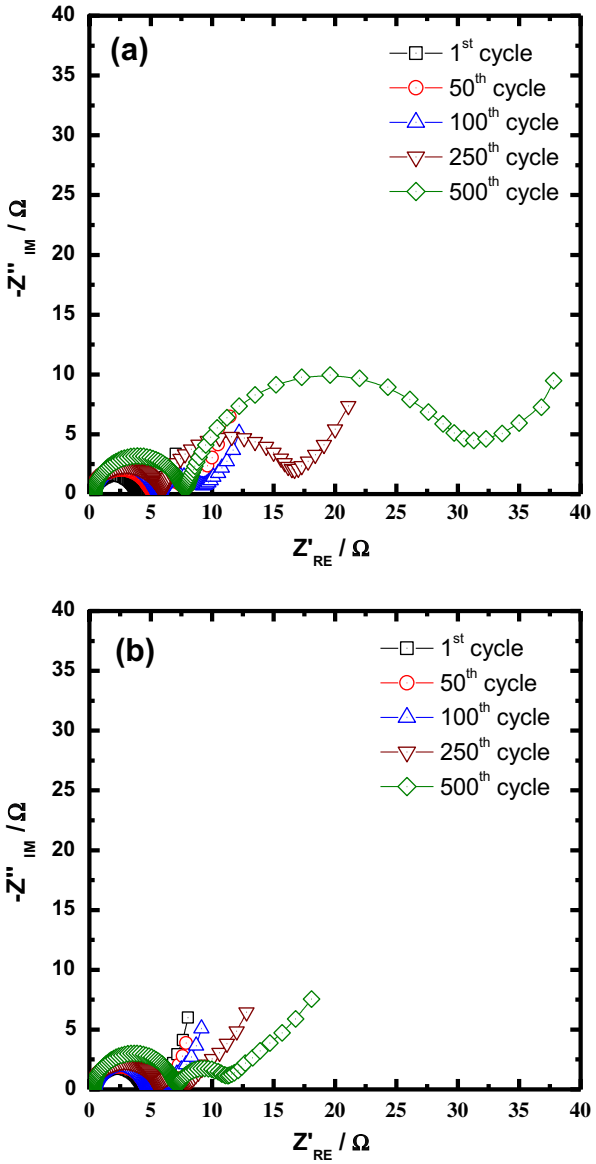

Fig. 7. Nyquist plots of (a) C/pristine $Li[Ni_{0.8}Co_{0.15}Al_{0.05}]O_2$ and (b) C/AlF_3-coated Li $[Ni_{0.8}Co_{0.15}Al_{0.05}]O_2$ cells charged at state to 4.2 V at 55 °C with respect to cycle number: 1st, 50th, 200th, 250th, 500th cycle.

Table 1
Surface-film resistance (R_{sf}) and charge-transfer resistance (R_{ct}) of pristine and AlF_3-coated $Li[Ni_{0.8}Co_{0.15}Al_{0.05}]O_2$according cycle number.

Cycle number	Pristine		AlF_3-coated	
	$Li[Ni_{0.8}Co_{0.15}Al_{0.05}]O_2$		$Li[Ni_{0.8}Co_{0.15}Al_{0.05}]O_2$	
	R_{sf} (Ω)	R_{ct} (Ω)	R_{sf} (Ω)	R_{ct} (Ω)
1	3.73	0.37	4.09	0.68
50	4.79	2.68	4.42	0.72
100	5.45	3.57	4.55	0.97
250	5.64	11.31	5.29	2.43
500	7.46	25.80	6.88	4.93

at 7 C, while the C/AlF_3-coated $Li[Ni_{0.8}Co_{0.15}Al_{0.05}]O_2$ cell had an outstanding capacity retention.

The AC impedance for C/pristine and AlF_3-coated $Li[Ni_{0.8}Co_{0.15}Al_{0.05}]O_2$ cells was measured as a function of cycle number in the fully charged state at 55 °C to understand the improved electrochemical performance of the AlF_3-coated $Li[Ni_{0.8}Co_{0.15}Al_{0.05}]O_2$, as shown in Fig. 7. The Nyquist plots show two semicircles, one in the high to medium frequency region which associated with the surface film resistance (R_{sf}) and the other in the low-frequency region resulting from charge transfer resistance (R_{ct}) coupled with a double-layer capacitance [18]. Variations in R_{sf} and R_{ct} for both cells at various cycles are shown in Table 1. The R_{sf} of both cells was very stable and almost unchanged during the cycling test, which confirmed the suspicion that the AlF_3 layer did not affect the surface resistance. In contrast to R_{sf}, the R_{ct} of C/pristine Li $[Ni_{0.8}Co_{0.15}Al_{0.05}]O_2$ increased rapidly with cycling though the R_{ct} (0.37 Ω) at the 1st cycle of the pristine cell was smaller than that (0.68 Ω) of the AlF_3-coated cell. After 500 cycles, the value settled at 25.8 Ω. However, the R_{ct} value of the C/AlF_3-coated $Li[Ni_{0.8}Co_{0.15}Al_{0.05}]O_2$ cell was limited to 4.93 Ω after 500 cycles.

Fig. 8a and c shows TEM bright field images of the pristine Li $[Ni_{0.8}Co_{0.15}Al_{0.05}]O_2$ electrode after 500 cycles. Most of the particles from the cycled pristine $Li[Ni_{0.8}Co_{0.15}Al_{0.05}]O_2$ contained large cracks as can be observed in Fig. 8a or were pulverized during cycling. The internal stress developed from the apparent structural degradation was large enough to develop cracks inside the individual particles or even to break the particles apart. The structural degradation was likely triggered by the slow dissolution of the transition metal ions at the particle surface resulting from HF attack [22,24]. Evidence for the HF attack and the resulting metal dissolution can be confirmed in Fig. 8c which shows the serrated particle surface resulting from the slow surface dissolution of the primary particle surface. Additionally, the uneven contrast in the primary particles suggested internal strain within each particle. The pulverization of the pristine cathode material would lead to a rapid deterioration of the cycle performance, which is in agreement with the cycling performance data in Figs. 4 and 5. In contrast, the cycled AlF_3-coated $Li[Ni_{0.8}Co_{0.15}Al_{0.05}]O_2$ electrode remained intact even after 500 cycles, as shown in Fig. 8b. In fact, no broken particles were observed by TEM. Fig. 8d clearly demonstrates the unblemished surface of the cycled AlF_3-coated Li $[Ni_{0.8}Co_{0.15}Al_{0.05}]O_2$ particle. It appeared that the AlF_3 coating was effective in minimizing the leaching of metal ions from the particle

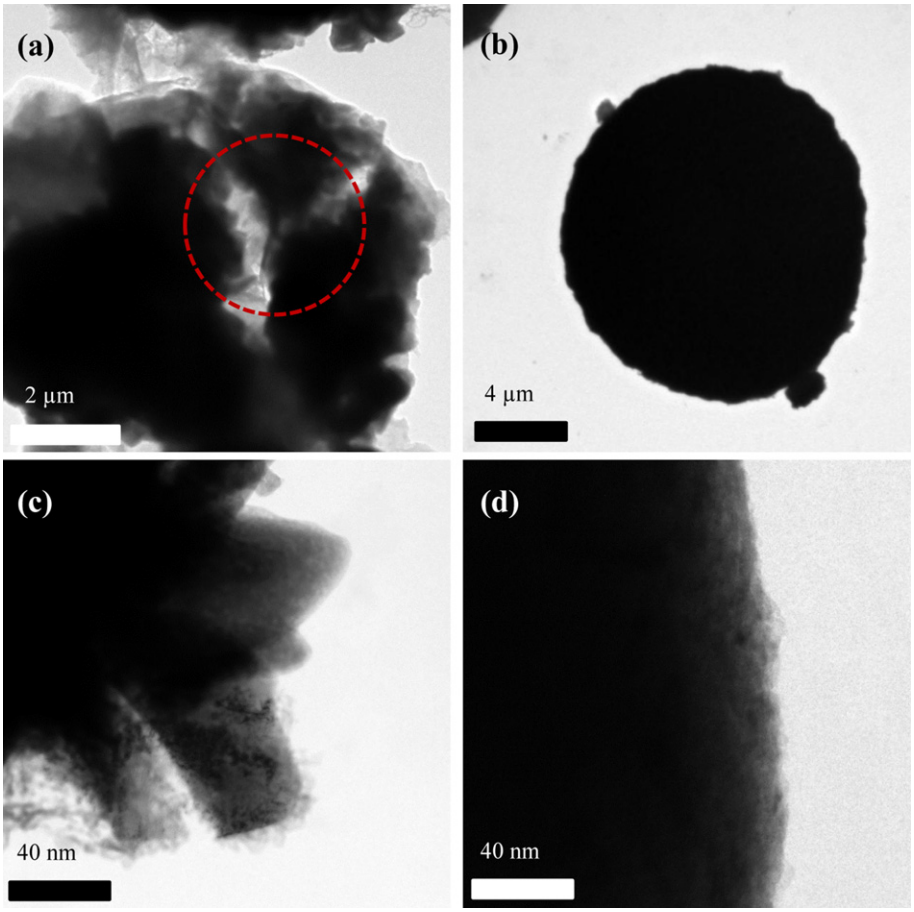

Fig. 8. TEM bright-field images of (a) the pristine $Li[Ni_{0.8}Co_{0.15}Al_{0.05}]O_2$, (c) magnified images of (a), (b) the AlF_3-coated $Li[Ni_{0.8}Co_{0.15}Al_{0.05}]O_2$, and (d) magnified images of (b) after 500 cycles at 55 °C.

surface and protecting the electrode from structural degradation, thus greatly improving the capacity of the $Li[Ni_{0.8}Co_{0.15}Al_{0.05}]O_2$ electrode. To confirm the above hypothesis, transition metal (Ni, Co, and Al) dissolution was measured and the result is shown in Fig. 9. The recovered active materials from the full cell charged 4.2 V were stored in the electrolyte at 55 °C and the dissolved transition metal ions into the electrolyte were analyzed with respect to storage time by ICP. As shown in Fig. 9, the dissolved amounts of Ni and Co for the pristine $Li_{1-\delta}[Ni_{0.8}Co_{0.15}Al_{0.05}]O_2$ were 0.56 and 0.09 ppm, respectively at the first week, then rapidly increased and reached 24.02 and 4.12 ppm after 4 weeks. On the other hand, the dissolved contents of Ni and Co from the AlF_3-coated electrodes were 0.39 and 0.07 ppm, respectively, and increased steadily with respect to time and reached 10.02 and 1.21 ppm after 4 weeks. This result clearly demonstrates that coating with AlF_3 on the cathode surface effectively suppresses metal dissolution, which is consistent with the results of cycling performance, AC impedance, and TEM.

Fig. 10 shows the differential scanning calorimetry of Li/pristine and Li/AlF_3-coated $Li[Ni_{0.8}Co_{0.15}Al_{0.05}]O_2$ cells charged to 4.3 V. The pristine $Li[Ni_{0.8}Co_{0.15}Al_{0.05}]O_2$ electrode exhibited an exothermic peak at 230.4 °C with heat generation of 520.4 J g^{-1}. While the AlF_3-coated $Li[Ni_{0.8}Co_{0.15}Al_{0.05}]O_2$ electrode showed the peak at 237 °C with a low heat generation of 458 J g^{-1}. The AlF_3 coating layer could protect the surface of the $Li[Ni_{0.8}Co_{0.15}Al_{0.05}]O_2$ from HF attack in the electrolyte which could reduce the oxygen release from the host structure. It is believed that the enhanced thermal stability could be ascribed to the protection effect of the AlF_3 coating layer, prohibiting the oxidized cathode from being directly contacted with electrolyte solution and thus suppressing the oxygen release and reactivity of the reactive Ni^{4+} ions [22].

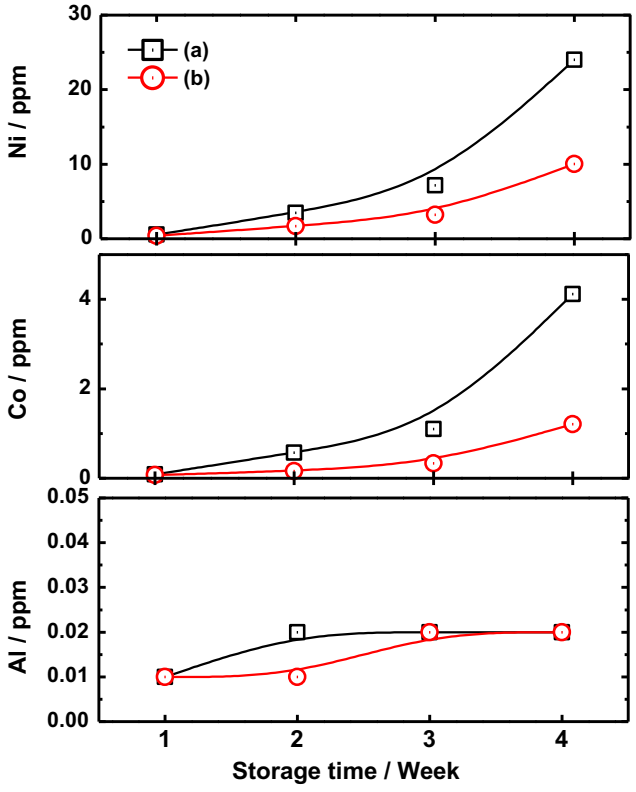

Fig. 9. Amount of dissolved Ni, Co, and Al after charging (a) pristine and (b) AlF_3-coated $Li[Ni_{0.8}Co_{0.15}Al_{0.05}]O_2$ electrodes to 4.2 V vs graphite. The electrodes were stored in fresh electrolyte (1 M $LiPF_6$ in EC:DEC = 1:1) at 55 °C for 4 weeks.

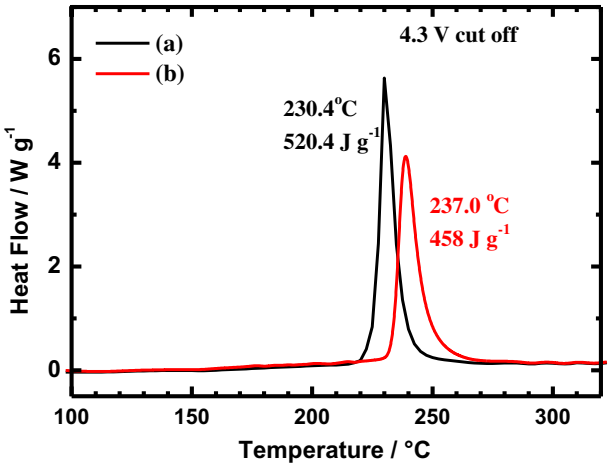

Fig. 10. Differential scanning calorimetry of (a) Li/pristine $Li[Ni_{0.8}Co_{0.15}Al_{0.05}O_2]$ and (b) Li/AlF_3-coated $Li[Ni_{0.8}Co_{0.15}Al_{0.05}]O_2$ cells charged to 4.3 V.

4. Conclusions

$Li[Ni_{0.8}Co_{0.15}Al_{0.05}]O_2$ surfaces were coated with a thick AlF_3 layer *via* a high-speed mechanofusion process to improve long-term cycling performance. The electrochemical study demonstrated that the AlF_3-coated $Li[Ni_{0.8}Co_{0.15}Al_{0.05}]O_2$ had better cycle durability, rate capability and thermal stability than pristine $Li[Ni_{0.8}Co_{0.15}Al_{0.05}]O_2$. Particularly, the C/$AlF_3$-coated $Li[Ni_{0.8}Co_{0.15}Al_{0.05}]O_2$ cell showed greatly improved capacity retention at an elevated temperature of 55 °C, showing a capacity retention of 55.9% after 500 cycles whereas that of the pristine electrode was only 11.7%. This improvement was mainly attributed to the following: 1) the protection of the electrode surface from HF attack in the electrolyte, a reduction of the dissolution of transition metal ions into the electrolyte, thereby suppressing an increase in the charge transfer resistance; and 2) the suppression of volume changes and thus preventing the cathode particle from being pulverized during cycling.

Acknowledgments

This work was supported by the National Research Foundation of Korea (NRF) grant funded by the Korea government (MEST) (No. 2009-0092780) and the Human Resources Development program (No. 20124010203290) of the Korea Institute of Energy Technology Evaluation and Planning (KETEP) grant funded by the Korea government Ministry of Knowledge Economy.

References

[1] X. Zhang, P.N. Ross, R. Kostecki, F. Kong, S. Sloop, J.B. Kerr, K. Striebel, E.J. Cairns, F. Mc Larnon, J. Electrochem. Soc. 148 (2001) A463–A470.
[2] J. Shim, R. Kostecki, T. Richardson, X. Song, K.A. Sriebel, J. Power Sources 112 (2002) 222–230.
[3] I. Belharouak, W. Lu, D. Vissers, K. Amine, Electrochem. Commun. 8 (2006) 329–335.
[4] R. Kostecki, F. McLarnon, Electrochem. Solid-State Lett. 7 (2004) A380–A383.
[5] M.-H. Kim, H.-S. Shin, D. Shin, Y.-K. Sun, J. Power Sources 159 (2006) 1328–1333.
[6] M. Guilmard, C. Pouillerie, L. Croguennec, C. Delmas, Solid State Ionics 160 (2003) 39–50.
[7] J.S. Weaving, F. Coowar, D.A. Teagel, J. Cullen, D.A. Dass, P. Bindin, R. Green, W.J. Macklin, J. Power Sources 97–98 (2001) 733–735.
[8] D.P. Abraham, R.D. Twesten, M. Balasubramanian, I. Petrov, J. McBreen, K. Amine, Electrochem. Commun. 4 (2002) 620–625.
[9] J. Cho, Y.J. Kim, B. Park, Chem. Mater. 12 (2000) 3788–3791.
[10] Z.H. Chen, J.R. Dahn, Electrochem. Solid-State Lett. 6 (2003) A221–A224.

[11] Y.-K. Sun, Y.-S. Lee, M. Yoshio, K. Amine, Electrochem. Solid-State Lett. 5 (2002) A99–A102.
[12] S.B. Jang, S.-H. Kang, K. Amine, Y.C. Bae, Y.-K. Sun, Electrochim. Acta 50 (2005) 4168–4173.
[13] Y.-K. Sun, J.-M. Han, S.-T. Myung, S.-W. Lee, K. Amine, Electrochem. Commun. 8 (2006) 821–826.
[14] Y.-K. Sun, S.-W. Cho, S.-W. Lee, C.S. Yoon, K. Amine, J. Electrochem. Soc. 154 (2007) A168–A172.
[15] A.T. Appapillai, A.N. Mansour, J. Cho, Y. Shao-Horn, Chem. Mater. 19 (2007) 5748–5757.
[16] D.-J. Lee, B. Scrosati, Y.-K. Sun, J. Power Sources 196 (2011) 7742–7746.
[17] Z. Chen, Y. Qin, K. Amine, Y.-K. Sun, J. Mater. Chem. 20 (2010) 7606–7612.
[18] Y.-K. Sun, S.-T. Myung, C.S. Yoon, D.-W. Kim, Electrochem. Solid-State Lett. 12 (2009) A163–A166.
[19] Y. Cho, J. Cho, J. Electrochem. Soc. 157 (2010) A625–A629.
[20] M.-H. Lee, Y.-J. Kang, S.-T. Myung, Y.-K. Sun, Electrochim. Acta 50 (2004) 939–948.
[21] W. Li, J.N. Reimers, J.R. Dahn, Solid State Ionics 67 (1993) 123–130.
[22] S.-U. Woo, C.S. Yoon, K. Amine, I. Belharouak, Y.-K. Sun, J. Electrochem. Soc. 154 (2007) A1005–A1009.
[23] S.-U. Woo, B.-C. Park, C.S. Yoon, S.-T. Myung, J. Prakash, Y.-K. Sun, J. Electrochem. Soc. 154 (2007) A649–A655.
[24] G.G. Amatucci, J.M. Tarascon, L.C. Klein, Solid State Ionics 83 (1996) 167–173.